# Theoretical Analyses of Band Engineered InGaAs/GaAsSb Double Quantum Well Nanostructure on InP Substrate (001) Using Transfer Matrix Method

Ugochukwu Joseph[1], Akwuegbu O.C[1]., Asiegbu A.D.[1], E.O.Ekpe[1] , Nwaokorongwu E.L[1].

*[1](Department of Physics, Michael Okpara University of Agriculture, Umudike, Umuahia, Nigeria)*

**Abstract**
*This paper gave a theoretical understanding of the transmission of symmetrical structure of InGaAs/GaAsSb double quantum well in InP substrate using transfer matrix method (TMM). Variation of the barrier width at a fixed proportion of the Indium concentration in InGaAs/GaAsSb which denotes the conduction band offset was studied with respect to the intensity of transmission reveals that the energy eigenvalues of the quantum well increases with increase in the width of the well with the least energy value obtained at the highest well width. The position peak shifts to the lower energy when the width of the well is increased, with value of 0.0381 eV to 0.0134 eV for well width of 10 nm to 20 nm respectively. With the effect of the electric field of about 0.1 eV, there was an improvement in thr transmittance of the heterstructure from 0.9073 to 0.9882 for well width from 10nm to 20 nm respectively. Effect of the energy on transmission coefficients considering tunneling effects were shown using the Matlab program to evaluate Transfer Matrix Method*
**Key Word**: *Conduction Band Offset, Strained Material, Transmission Probability, Transfer Matrix.*

---------------------------------------------------------------------------------------------------------------------------------
---------------------------------------------------------------------------------------------------------------------------------

## I.    Introduction

In today's modification in the advancement in epitaxial growth of heterostructures, several materials have been fabricated having wide applications in different variety of fields at respective wavelength [1,2] .Effort has been done on the study of III-V direct bandgaps alloys due to their applications to optoelectronic devices. Attention has been paid on AlGaAs/GaAs because of closeness in their lattice parameters and its negligible strain effects. These heterostructures can be used for advance electronic devices like optical components, resonant tunneling devices, optoelectronic devices etc. Most importantly is its use in optical and optoelectronic purposes. High level devices are achievable because of the growth in microelectronics technology [3]. Multiple quantum well (MQW) formed by two or more identical or different QWs allow carrier tunneling when they have narrow potential barrier. An exciton can be formed by an electron and a hole provided there is wide potential barrier.  In these cases, wave functions originating from one QW extend into the other QW, meaning electron or hole lies in both QWs simultaneously, having different quantum probabilities [4]. In order to be able to design such high/superior photo-dectators, the use of theoretical approach is necessary with enough level of accuracy to estimate the confined quantum well energy level and the respective wave functions. That is the (the characteristic roots and vectors). The wavelength detected by a device using interband and intersubband transition can be estimated accurately [5].

Quantum well can be understood through the simple "particle-in-a box" model, considering Schrödinger's equation in one dimension for the particle of interest (e.g., electron or hole). Solving 1D Schrodinger equation, one can use a numerical method known as Transfer matrix method. It gives exact solution for system of functions whose potential are in series arbitrarily[6]. Investigating the quantum mechanical tunneling in a quantum well, transmission coefficient is extracted from the solution to the one dimensional time independent Schrödinger equation. The transmission coefficient is obtained by the ratio of the flux of particles penetrating a potential barrier to the flux of particle incident on the barrier. [7].

The main objective of the paper is to study behavior of wave functions in the quantum wells and their overlapping with adjacent wells if thickness of InGaAs/GaAsSb barrier region is reduced. The barrier widths have been optimized for the better quantum confinement for the varying number of wells. In this paper, we present investigation of wave function intensities along with their surface images and effect of barrier thickness in nanostructures. The wave function intensity has been calculated by squaring wave function amplitude for the varying some numbers of wells. Transfer matrix method (TMM) [8], a simple and accurate numerical method was used to obtain solutions of Schrodinger equation in well and barrier regions. The simulation was carried out

---

using MATLAB software. Transmission coefficients have been determined for nanostructure structures with varying mole fraction. Furthermore, we deduced the bound state energy as a function of variation in effective mass of electron in the barrier and barrier height with aluminum concentration for both the nanostructures. The computational efforts needed to compute energy through secant method has been simulated in terms of number of iterations [9].

## II. Material And Methods

Using the transfer matrix method, we studied the $In_xGa_{1-x}As/GaAs_{0.51}Sb_{0.49}$ heterostuctures. We consider a quantum well constituted by two semiconductor material $In_xGa_{1-x}As$ and $GaAs_{0.51}Sb_{0.49}$.

Considering the motion of a quantum particle of mass, m, with a rectangular barrier of height presence of V (z) in the z direction as shown in the figure below
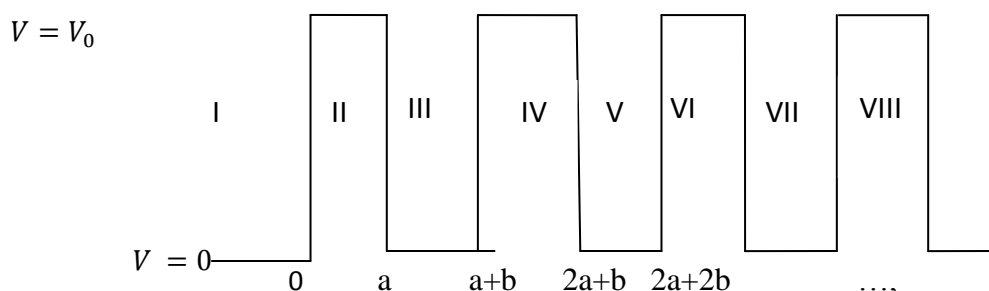


**Figure 1:** Quantum structure wıtn ınfinite well

By the Schrodinger equation and assuming the energy incident on the electrons and holes is less than the potential $V_0$, we have,

$$\frac{h^2}{8\pi^2 m(z)}\frac{\partial^2\psi}{\partial z^2} + [V(z) - E]\psi(z) = 0 \tag{1}$$

where $\psi$ is the *wave function,* V(z) is the potential function and $E$ the energy of the electron. The general solution of the Schrödinger equation in each region is

$$\psi_1(z) = Ee^{i\beta_1 z} + Fe^{-i\beta_1 z} \text{ (z<0)} \tag{2}$$

$$\psi_2(z) = Ge^{\beta_2 z} + He^{-\beta_2 z} \text{ (0<z<a)} \tag{3}$$

$$\psi_3(x) = Ie^{i\beta_1 z} + Je^{-i\beta_1 z} \quad \text{(a<z)} \tag{4}$$

$$\psi_4(z) = Ke^{\beta_2 z} + Le^{-\beta_2 z} \text{ (0<z<a)} \tag{5}$$

where $\beta_1 = \sqrt{8\pi^2 m(z)E/h^2}$ and $\beta_2 = \sqrt{8\pi^2(E - V_0)/h^2}$. \hfill (6)

Applying the BenDaniel-Duke boundary conditions for continuity of wave functions [10] i.e.
$\psi_1 = \psi_2$ at $z = 0$ and $\frac{1}{m_w}\frac{d\psi_{1(0)well}}{dz} = \frac{1}{m_b}\frac{d\psi_{2(0)barrier}}{dz}$ at the interface of the two materials, where $m_b$ and $m_w$ are the mass of the barrier and well respectively, we have

$$E + F = G + H \tag{7}$$

and

$$i\beta_1\frac{1}{m_w}E - \frac{1}{m_w}i\beta_1 F = \frac{1}{m_b}\beta_2 G - \frac{1}{m_b}\beta_2 H \tag{8}$$

In matrix notation, it is written as

$$\begin{bmatrix} 1 & 1 \\ \frac{i\beta_1}{m_b} & \frac{-i\beta_1}{m_b} \end{bmatrix}\begin{bmatrix} E \\ F \end{bmatrix} = \begin{bmatrix} 1 & 1 \\ \frac{\beta_2}{m_w} & -\frac{\beta_2}{m_w} \end{bmatrix}\begin{bmatrix} G \\ H \end{bmatrix} \tag{9}$$

$$\begin{bmatrix} E \\ F \end{bmatrix} = \frac{1}{2}\begin{bmatrix} 1 + \frac{m_w}{m_b}\frac{\beta_2}{i\beta_1} & 1 - \frac{m_w}{m_b}\frac{\beta_2}{i\beta_1} \\ 1 - \frac{m_w}{m_b}\frac{\beta_2}{i\beta_1} & 1 + \frac{m_w}{m_b}\frac{\beta_2}{i\beta_1} \end{bmatrix}\begin{bmatrix} G \\ H \end{bmatrix} \tag{10}$$

Similarly, taking regions two and three and observing all the boundary conditions at $z = a$, we have

$$\begin{bmatrix} G \\ H \end{bmatrix} * \begin{bmatrix} e^{\beta_2 a} & e^{-\beta_2 a} \\ \frac{\beta_2}{m_w}e^{\beta_2 a} & -\frac{\beta_2}{m_w}e^{\beta_2 a} \end{bmatrix} = \begin{bmatrix} I \\ J \end{bmatrix} * \begin{bmatrix} 1 & 1 \\ \frac{i\beta_1}{m_b} & -\frac{i\beta_1}{m_b} \end{bmatrix} \tag{11}$$

$$\begin{bmatrix} G \\ H \end{bmatrix} = \frac{1}{2} \begin{bmatrix} \left(1 + \frac{m_b}{m_w}\frac{i\beta_1}{\beta_2}\right)e^{-\beta_2 a + i\beta_1 a} & \left(1 - \frac{m_b}{m_w}\frac{i\beta_1}{\beta_2}\right)e^{-\beta_2 a - i\beta_1 a} \\ \left(1 - \frac{m_b}{m_w}\frac{i\beta_1}{\beta_2}\right)e^{\beta_2 a + i\beta_1 a} & \left(1 + \frac{m_b}{m_w}\frac{i\beta_1}{\beta_2}\right)e^{\beta_2 a - i\beta_1 a} \end{bmatrix} \begin{bmatrix} I \\ J \end{bmatrix} \quad (12)$$

For regions three and four, and observing all the boundary conditions at $z = a + b$ we have;

$$\begin{bmatrix} I \\ J \end{bmatrix} * \begin{bmatrix} e^{\beta_2(a+b)} & e^{-\beta_2(a+b)} \\ \frac{\beta_2}{m_w}e^{\beta_2(a+b)} & -\frac{\beta_2}{m_w}e^{\beta_2(a+b)} \end{bmatrix} = \begin{bmatrix} K \\ L \end{bmatrix} * \begin{bmatrix} e^{i\beta_1(a+b)} & e^{-i\beta_1(a+b)} \\ \frac{i\beta_1}{m_b}e^{\beta_2(a+b)} & \frac{-i\beta_1}{m_b}e^{\beta_2(a+b)} \end{bmatrix}$$

$$\begin{bmatrix} I \\ J \end{bmatrix} = \frac{1}{2} \begin{bmatrix} \left(1 + \frac{m_w}{m_b}\frac{\beta_2}{i\beta_1}\right)e^{-i\beta_1(a+b)+\beta_2(a+b)} & \left(1 - \frac{m_w}{m_b}\frac{\beta_2}{i\beta_1}\right)e^{-i\beta_1(a+b)-\beta_2(a+b)} \\ \left(1 - \frac{m_w}{m_b}\frac{\beta_2}{i\beta_1}\right)e^{i\beta_1(a+b)+\beta_2(a+b)} & \left(1 + \frac{m_w}{m_b}\frac{\beta_2}{i\beta_1}\right)e^{i\beta_1(a+b)-\beta_2(a+b)} \end{bmatrix} * \begin{bmatrix} K \\ L \end{bmatrix} \quad (13)$$

Observing the alphabetical sequences for the constants if we decide to go for more regions at $z = 2a + b, 2a + 2b$ and $3a + 2b$, we have

$$\begin{bmatrix} K \\ L \end{bmatrix} = \frac{1}{2} \begin{bmatrix} \left(1 + \frac{m_b}{m_w}\frac{i\beta_1}{\beta_2}\right)e^{-\beta_2(2a+b)+i\beta_1(2a+b)} & \left(1 - \frac{m_b}{m_w}\frac{i\beta_1}{\beta_2}\right)e^{-\beta_2(2a+b)-i\beta_1(2a+b)} \\ \left(1 - \frac{m_b}{m_w}\frac{i\beta_1}{\beta_2}\right)e^{\beta_2(2a+b)+i\beta_1(2a+b)} & \left(1 + \frac{m_b}{m_w}\frac{i\beta_1}{\beta_2}\right)e^{\beta_2(2a+b)-i\beta_1(2a+b)} \end{bmatrix} * \begin{bmatrix} M \\ N \end{bmatrix} \quad (14)$$

$$\begin{bmatrix} M \\ N \end{bmatrix} = \frac{1}{2} \begin{bmatrix} \left(1 + \frac{m_w}{m_b}\frac{\beta_2}{i\beta_1}\right)e^{-i\beta_1(2a+2b)+\beta_2(2a+2b)} & \left(1 - \frac{m_w}{m_b}\frac{\beta_2}{i\beta_1}\right)e^{-i\beta_1(2a+2b)-\beta_2(2a+2b)} \\ \left(1 - \frac{m_w}{m_b}\frac{\beta_2}{i\beta_1}\right)e^{i\beta_1(2a+2b)+\beta_2(2a+2b))} & \left(1 + \frac{m_w}{m_b}\frac{\beta_2}{i\beta_1}\right)e^{i\beta_1(2a+2b)-\beta_2(2a+2b)} \end{bmatrix} * \begin{bmatrix} O \\ P \end{bmatrix} (15)$$

If the reflection coefficient is zero for the last region, we have

$$\begin{bmatrix} M \\ N \end{bmatrix} = \frac{1}{2} \begin{bmatrix} \left(1 + \frac{m_w}{m_b}\frac{\beta_2}{i\beta_1}\right)e^{-i\beta_1(2a+2b)+\beta_2(2a+2b)} & 0 \\ \left(1 - \frac{m_w}{m_b}\frac{\beta_2}{i\beta_1}\right)e^{i\beta_1(2a+2b)+\beta_2(2a+2b))} & 0 \end{bmatrix} * \begin{bmatrix} O \\ P \end{bmatrix}$$

For double barrier, we have

$$\begin{bmatrix} K \\ L \end{bmatrix} = \frac{1}{2} \begin{bmatrix} \left(1 + \frac{m_b}{m_w}\frac{i\beta_1}{\beta_2}\right)e^{-\beta_2(2a+b)+i\beta_1(2a+b)} & 0 \\ \left(1 - \frac{m_b}{m_w}\frac{i\beta_1}{\beta_2}\right)e^{\beta_2(2a+b)+i\beta_1(2a+b)} & 0 \end{bmatrix} * \begin{bmatrix} M \\ N \end{bmatrix} \quad (16)$$

where M is the Transmittance. The transmission coefficient P is then given as

$$P = M = \frac{|E|^2}{|W|^2} \quad (17)$$

While the reflection coefficient F=R would be given by

$$F = R = YM = Y\left(\frac{E}{W}\right) \quad (18)$$

### III. Result and Discussion

Investigating the transmission and the reflectance coefficients of two symmetric well structures without any external field, the mass of the barrier is given as

$$m_b = 0.51(0.067) + 0.49(0.039) = 0.533m_0$$

while the mass of the well changes based on the mole ratio of the constituent compounds. The table below gives the conduction band offset for different molar concentration of Indium Arsenide in Gallium Indium Arsenide using the solid model theory

**Table 1:** Band offsets values at different symmetric well masses

| Composition of Indium (x) | Mass of the well | Unstrained conduction Band Offset (eV) | Strained conduction band offset (eV) |
|---|---|---|---|
| 0.53 | 0.0475 | 0.1929 | 0.1960 |
| 0.55 | 0.0467 | 0.2080 | 0.2020 |
| 0.60 | 0.0446 | 0.2439 | 0.2158 |
| 0.65 | 0.0424 | 0.2770 | 0.2282 |
| 0.70 | 0.0402 | 0.3073 | 0.2395 |
| 0.75 | 0.0380 | 0.3348 | 0.2496 |
| 0.80 | 0.0357 | 0.3595 | 0.2588 |
| 0.85 | 0.0333 | 0.3814 | 0.2670 |
| 0.90 | 0.0309 | 0.4006 | 0.2744 |
| 0.95 | 0.0285 | 0.4169 | 0.2810 |
| 1.00 | 0.0260 | 0.4305 | 0.2870 |

Table 1 and figure 2 show that as the composition of Indium is increased in InGaAs, the conduction band offset increases. When the material was strained on InP, the conduction band offset changed from 0.1929 to 0.1960 eV at 0.53 composition (concentration) of Indium in InGaAs.

For double barrier system, the tunneling energy was found to be increasing with increase in the composition of Indium in InGaAs with decrease in the mass of the well. The energy was found to increase from 0.1960eV to 0.2870eV.
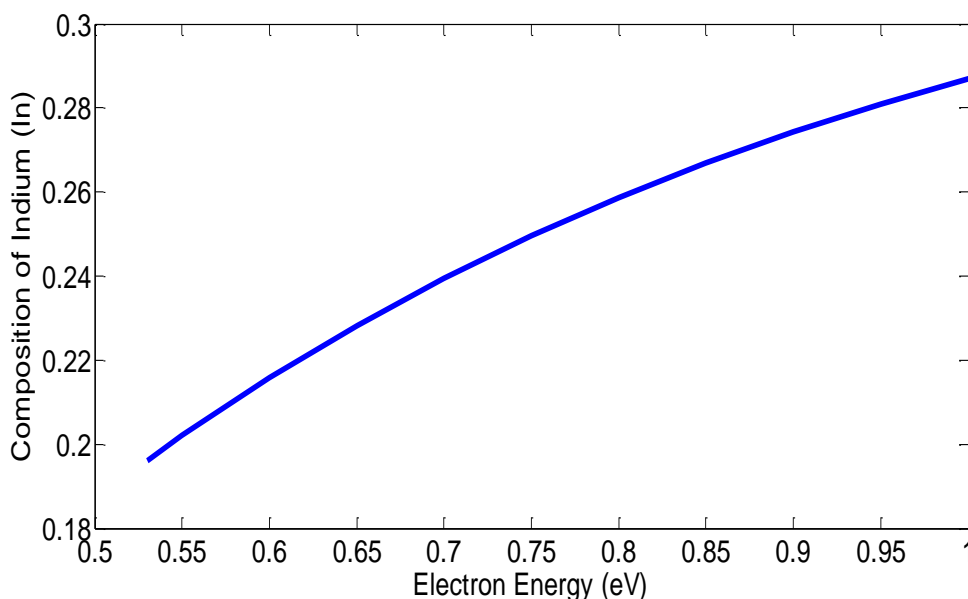


**Figure 2:** Variation of the Composition of Indium in InGaAs with energy

Varying the width of the well from 10nm to 20nm at 2nm interval with the band offset of 0.1920 and 0.1960 eV, for unstrained and strained InGaAs, we observed from Figs.3 and 4 that with increase in the width of the well, there was more confinement of electrons in the well with decrease in the transmission for both strained and unstrained material. The transmission probability increases with increase in the conduction band offset due to the increase in the composition of Indium in GaInAs. The energy eigen values of the quantum well increases with increase in the width of the well with the least energy value obtained at the highest well width. The position peak shifts to the lower energy when the width of the well is increased. Since the energy is less than the conduction band potential, energies are confined in the well.
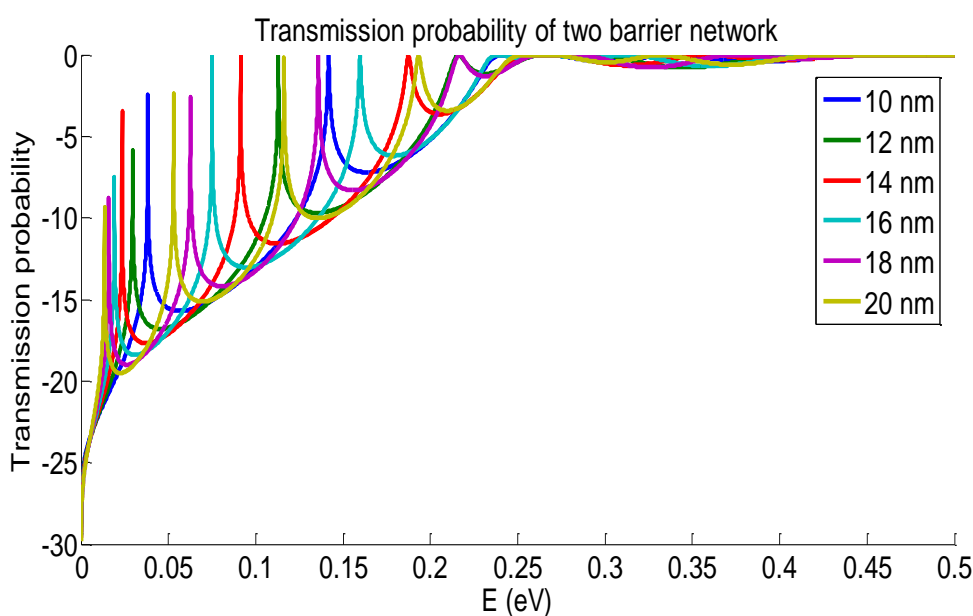


**Figure 3:** Variation of the transmission probability with energy at varying well width for strained InGaAs
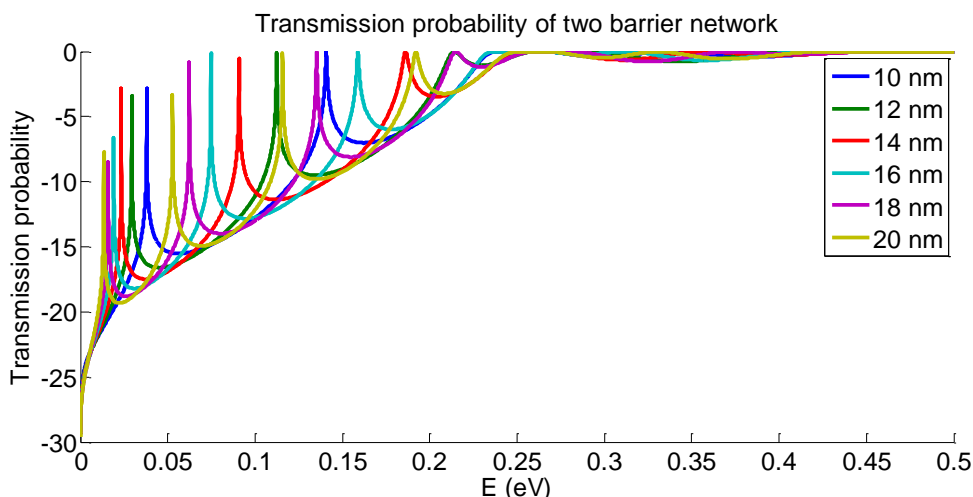
**Figure 4:** Variation of the transmission probability with energy at varying well width for unstrained InGaAs

**Table 2:** Well width variation with energy Eigen values

| Well width in nm | Energy Eigen Value (eV) | | | |
|---|---|---|---|---|
| | $E_1$ (eV) | $E_2$(eV) | $E_3$(eV) | $E_4$(eV) |
| 10 nm | 0.0381 | 0.1417 | --- | --- |
| 12 nm | 0.02955 | 0.1131 | | --- |
| 14 nm | 0.0236 | 0.09141 | 0.1877 | --- |
| 16 nm | 0.01915 | 0.07506 | 0.1601 | --- |
| 18 nm | 0.0159 | 0.06266 | 0.1359 | |
| 20 nm | 0.0134 | 0.05301 | 0.1162 | 0.1935 |

Table 2 gives the summary of Eigen-values of the confined electrons at increasing well width of InGaAs for 0.1960 eV conduction band offset of the heterojunction of $In_{0.53}Ga_{0.47}As/GaAs_{0.51}Sb_{0.49}$ strained on *InP*. With the well width of 10 nm, only two Eigen states existed. But with increase in the barrier well width of the heterostructure, the energy Eigen states increased. These results are comparable to the finite well system

Varying the thickness of the barrier from 10nm to 20 nm at interval of 2nm, we observe that the increase in the width of the well has no effect on the Eigen values of the quantum well. That is, there was no shift in the Eigen values but on the tunneling through the barrier. The peak of every value decreases with increase in the thickness of the barriers. This can be illustrated in Figs.5. The band offset was set at 0.1960 eV. The tunneling of electrons through the potential barrier was seen to increase with increase in the width of the well. Figure 6 reveals that at 0.1960 eV and higher conduction band offset, there was a non-zero transmission probability with little increase with respect to the energy of the photon.
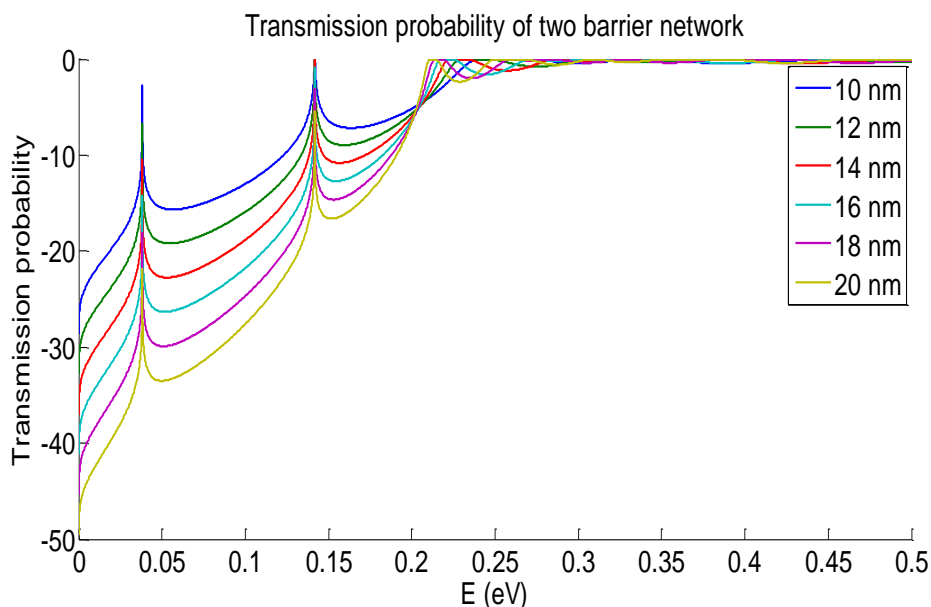


**Figure.5:** Variation of the transmission probability with energy at varying thickness of barrier
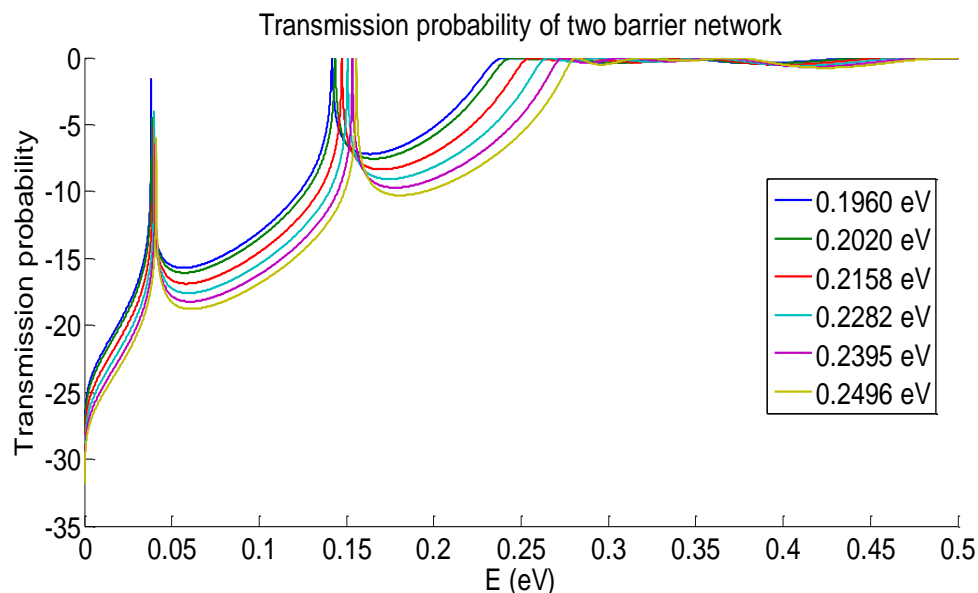
**Figure 6:** Variation of the transmission probability with energy at variation of conduction band offset for strained InGaAs at 10 nm well width

With the effect of the electric field 0f 0.1 eV through the heterostructure, there is varying changing in the transmittance and the reflectance through the walls of the barrier. Figures 7, 8 and 9 illustrates the various changes as a result of changes in the barrier thickness, changes in the width of the well and also the changes in the band offset of the heterostructure for transmittance and reflectance
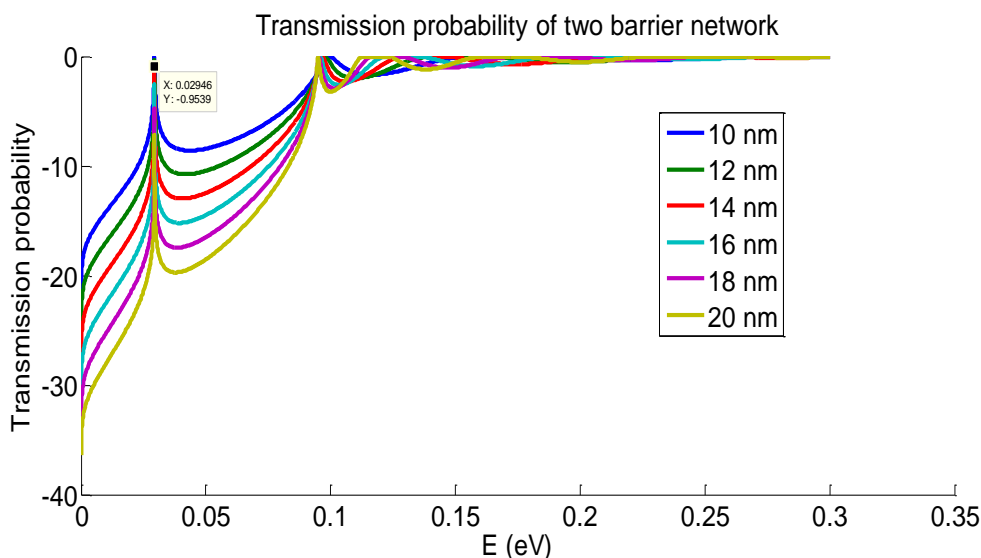


Figure 7: Variation of the transmission Probability as a function of Energy at varying thickness of the barrier when passed through an electric field of 0.1 eV
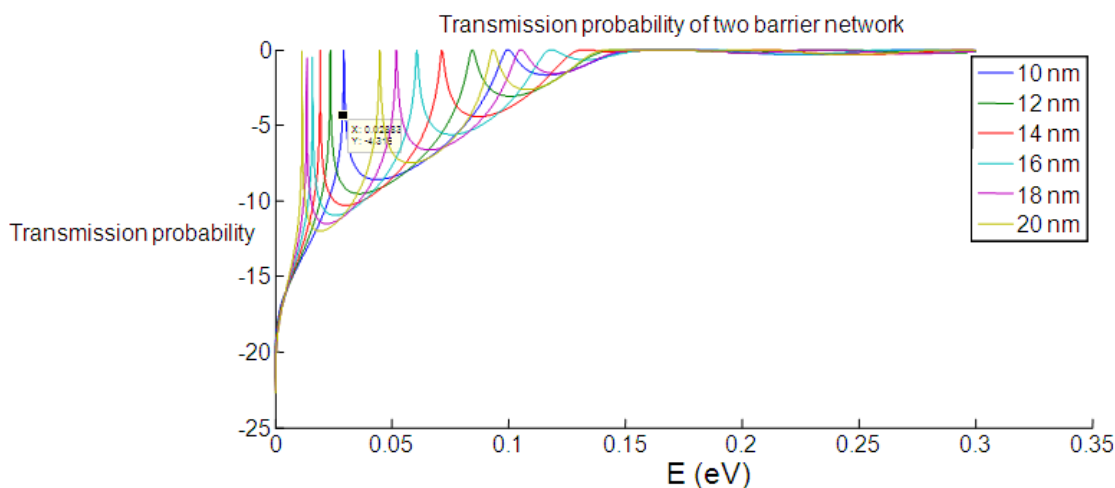
**Figure 8:** Variation of the transmission Probability as a function  for varying amount of well depth
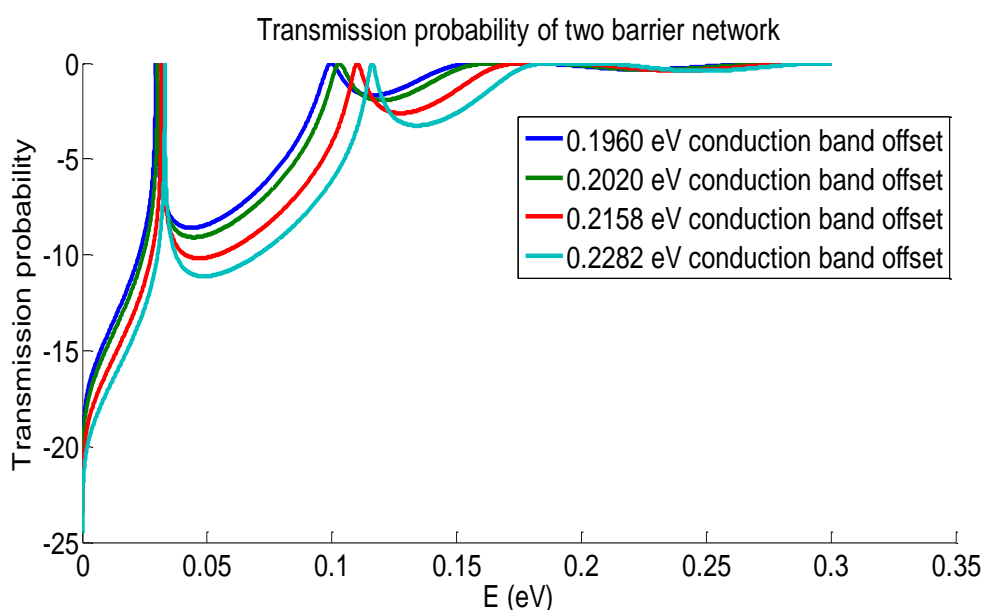


Figure 9: Variation of the transmission Probability as a function of conduction band offset

The transmittance goes in a sinusoidal increase with its maximum at 0.9970 for barrier thickness changes from 10 nm to 20 nm.  The reflectance reduces from 0.0297 at 10nm to 0.0379 at 20 nm barrier thickness.
With increase in the width of the well from 10nm to 20nm, it was observed that the transmittance increases from 0.9703 to 0.9882 while there was an increase in the decrease of the reflectance of the heterostructure when the band offset was increased which increased from 0.1960 to 0.2282 for well width of 10 nm

## IV. Conclusion
The wave function intensity, energy and transmission probability in a double quantum well were studied using transfer matrix method (TMM). The effect of Indium composition in InGaAs in the well region was considered by varying the conduction band offset in the analysis. The increase and reduction in the barrier thickness and well width were simulated to study the confinement energy and the tunneling effect in one direction.

## References
[1].    Fissel A., Schröter B, Kaiser U, Richter W, (2000)  Advance in the molecular beam epitaxial growth of artificially  layered heteropolytypic structure of SiC. *Appl. Phys. Lett*. 77, 2418–2420
[2].    Rogalski A, 2002 'Infrared detectors: an overview  Elsevier *Infrared Physics & Technology*. 43 ,P. 187–210.
[3].    Shreyasi Mukherjee, Arpan Deyasi, Avishek Roy, Souvik Kundu, Soma Gharami, (2014) calculating transmission coefficient of Double triangular quantum well electric field for different structural parameters. IJRASET Vol. 2 Issue IV, April 2014 ISSN: 231-9653

[4].    Miller D. A. B, Weiner J. S, and Chemla D. S.,(1986) 'Electric field Dependence of Linear Optical Properties in Quantum Well Structures: Waveguide Electroabsorption and Sum Rules.' *IEEE J. Quantum Electron*. QE-22, 1816-1830

[5].    Ricardo A. Tavares Santos, Fábio Durante P. Alves, Christian G. R. Taranti, Jayr de Amorim Filho, Gamani Karunasiri (2008). QWIP DESIGN: An Approach Using The Transfer Matrix Method To Calculate The Bound States In Valence And Conduction Band X Simposio de Aplicacoes Operacionais em Areas de Defesa, ITA-Sao Jose dos Campos, SP 24-26

[6].    James S, Walker and Gathright J., (1992) ' A transfer-matrix approach to one- dimensional quantum mechanics using Mathematica'. Computers in Physics 6, *American Institute of Physics*, 393-399 https://doi.org/10.1063/1.168430

[7].    Dairi M., Brezini A., Zanoun A., (2018) ' Electronic Properties of Semiconductor Supperlattices: Numerical Study of Dimer Effect . Bulg. J. Phys. 45,  247-254

[8].    Talele K, Patil D.S.,(2008) Analysis of wave function, energy and Transmission Coefficient in GaN/AlGaN Supperlattice Nanostructure. Progress In Electromagnetics Research, PIER 81, 237-252

[9].    Djelti R., Bentata S., Aziz Z., Besbes A.,(2012), Mixed disorder in GaAs/Al$_x$Ga$_{1-x}$ As superlattices and its effect on the range of wavelength infrared lasers; Elsevier, Optik 124 (2013) 3812– 3815

[10].    Noteborn, H. J. M. F. (1993). Quantum tunneling transport of electrons in double-barrier heterostructures: theory and modeling. Technische Universiteit Eindhoven. https://doi.org/10.6100/IR396859